Available online at www.sciencedirect.com
SCIENCE DIRECT®
Journal of Magnetic Resonance 177 (2005) 139–145
JMR Journal of Magnetic Resonance
www.elsevier.com/locate/jmr

Increasing the sensitivity of time-resolved photo-CIDNP experiments by multiple laser flashes and temporary storage in the rotating frame

Martin Goez [a,*], Ilya Kuprov [b], P.J. Hore [b,*]

[a] Fachbereich Chemie, Martin-Luther-Universität Halle-Wittenberg, Kurt-Mothes-Strasse 2, D-06120 Halle/Saale, Germany
[b] Department of Chemistry, University of Oxford, Physical and Theoretical Chemistry Laboratory, South Parks Road, Oxford OX1 3QZ, UK

Received 10 March 2005; revised 27 May 2005
Available online 24 August 2005

Abstract

Pulse sequences have been developed that add up time-resolved photo-CIDNP signals from n successive laser flashes not in the acquisition computer of the NMR spectrometer but in the experiment itself, resulting in a greatly improved signal-to-noise ratio. For this accumulation, CIDNP is first stored in the transverse plane and then on the z axis, and finally superimposed on CIDNP produced by the next flash. These storage cycles also result in a very efficient background suppression. Because only one free induction decay is acquired for n flashes, the noise is digitized only once. The signal gain is demonstrated experimentally and analyzed theoretically. Losses are mostly due to nuclear spin relaxation, and to a small extent to instrument imperfections. With 10 laser flashes, a signal increase by a factor of about 7.5 was realized. As their main advantage compared to signal averaging in the usual way, these sequences yield the same signal-to-noise ratio with fewer laser flashes; the theoretical improvement is by a factor of $\sqrt{n}$.

Keywords: Chemically induced dynamic nuclear polarization; Pulse sequences; Signal-to-noise ratio; Laser methods; Photoinduced electron transfer

1. Introduction

Sensitivity is much more of an issue with NMR than with most other spectroscopic methods because the magnetic interactions are so weak. A great many technological and methodological developments of NMR have been motivated by the quest for improved signal-to-noise ratios. The most important of these is Fourier transform NMR itself, which was originally introduced for the sole purpose of increasing the sensitivity [1], almost a decade having to pass until coherence transfer was recognized as its even more valuable benefit [2].

Chemically induced dynamic nuclear polarization (CIDNP) [3] is an effect that produces enhanced NMR signals by creating nonequilibrium populations of the nuclear spin states in the products of a chemical reaction carried out in the field of the NMR magnet. Its operating principle, the so-called radical pair mechanism [4,5], relies on the interplay of nuclear-spin selective intersystem crossing and electron-spin selective chemical reactivity of radical pairs, and sorts the nuclear spins between different products. Because the signal amplification can be quite substantial but occurs only for molecules that have radical pairs as their precursors, those molecules can be observed selectively and discriminated against the background of unreacted molecules or

* Corresponding authors. Fax: +49 345 5527345 (M. Goez), +44 1865 275410 (P.J. Hore).
E-mail addresses: goez@chemie.uni-halle.de (M. Goez), peter.hore@chem.ox.ac.uk (P.J. Hore).

1090-7807/$ - see front matter © 2005 Elsevier Inc. All rights reserved.
doi:10.1016/j.jmr.2005.06.017

molecules formed by other pathways. There have been numerous applications of CIDNP to the elucidation of reaction mechanisms [6] and of molecular structures, including radicals [7–9] and biomolecules [10,11].

One intriguing aspect of the radical pair mechanism is that CIDNP is generated only during the radical-pair life, that is on a (sub)nanosecond timescale, but that the polarizations, once having arrived in the diamagnetic products, persist for a time on the order of T_1, 0.1...10 s for protons. This opens up the possibility of carrying out time-resolved CIDNP experiments [12,13] by initiating a reaction with a nanosecond laser flash and sampling the resulting polarizations with a radiofrequency (RF) pulse after a variable delay. On the timescale of NMR pulses, nanosecond events are immeasurably fast, but radical pair formation by bimolecular quenching of the electronically excited state and product formation by reactions of escaped radicals often fall into the microsecond domain and can be followed in that way, which extends the timescale of kinetic NMR by several orders of magnitude. Because the stable diamagnetic products are detected rather than the paramagnetic intermediates, there is no lifetime broadening, and because the radicals typically disappear on a timescale of about 100 μs, there is no appreciable paramagnetic broadening of the product signals.

Despite the signal enhancement by the polarizations, time-resolved CIDNP experiments are severely limited by the signal-to-noise ratio, which can be traced to the fact that the attainable concentration of radical pairs is a small fraction of the substrate concentration only. This is normally inevitable because of other constraints, but even in cases where it could be circumvented, the success of such an approach seems doubtful because very high radical concentrations will open up additional reaction channels, and thus distort the kinetics.

In this work, we present a feasible solution that uses several laser flashes per acquisition. The radical concentration problem is avoided because each new flash is applied at a time when the radicals from the preceding flash have already disappeared. The time-dependent polarizations generated by each flash are sampled with an RF pulse, stored between the flashes in a suitable way, and added up constructively; the accumulated polarization from n flashes is finally detected. Hence, the noise is the same as in an experiment with a single flash but the signal is approximately n times stronger.

2. Experimental

The CIDNP measurements were carried out on a 600 MHz (14.1 T) Varian INOVA NMR spectrometer. A frequency tripled (355 nm) Spectra-Physics GCR-130 Nd:YAG laser was used for sample illumination. Technical details of our time-resolved CIDNP experiment will be published separately.

All chemicals were obtained commercially in the highest available purity and used as received.

3. Results and discussion

3.1. Basic concepts

The issue of storing the polarizations between flashes in a time-resolved CIDNP measurement can be addressed as follows.

On the timescale accessible by the experiment ($\gtrsim$ 100 ns), the polarizations are essentially frozen in the diamagnetic products, so any time dependence observed invariably means that new diamagnetic molecules bearing polarizations have arrived on the scene. This is intuitively obvious for CIDNP increasing with time but we stress that it also holds for CIDNP decreasing with time: such a decrease does not indicate that diamagnetic molecules bearing polarizations have been *destroyed* but, on the contrary, that further molecules of the same type but bearing polarizations opposite to those already present, have been *formed*.

This has three implications.

First, as long as there is a time dependence of the polarizations, storage of CIDNP on the z axis is impossible because it would be obliterated by CIDNP arriving later, but storage in the transverse plane is perfectly feasible because coherences are left unchanged by later CIDNP events; for the latter reason, the value stored is the polarization present *at the moment* of the storing pulse. Indeed, the normal time-resolved CIDNP experiment performs exactly that storage but detects the result immediately.

Second, once the reaction is completed, i.e., CIDNP no longer changes, which usually means after a few hundreds of microseconds at most, storage on the z axis can be done as well, and for longer storage times is preferable to storage in the transverse plane because there is no evolution under homonuclear J couplings. Therefore, we restore CIDNP from the transverse plane to the z axis as soon as that is feasible.

Third, that constant magnetization stored on z and the time-dependent CIDNP from the next laser flash are simply superimposed, so the subsequent sampling pulse (applied at the same post-flash time as the previous one) takes both to the transverse plane.

The described procedure can be applied repeatedly; finally, the stored sum of CIDNP from a series of flashes with the same timing is read out and acquired. The development of longitudinal and transverse magnetization during such a multiflash experiment is depicted schematically in Fig. 1. The background of unreacted molecules does not interfere with this method because

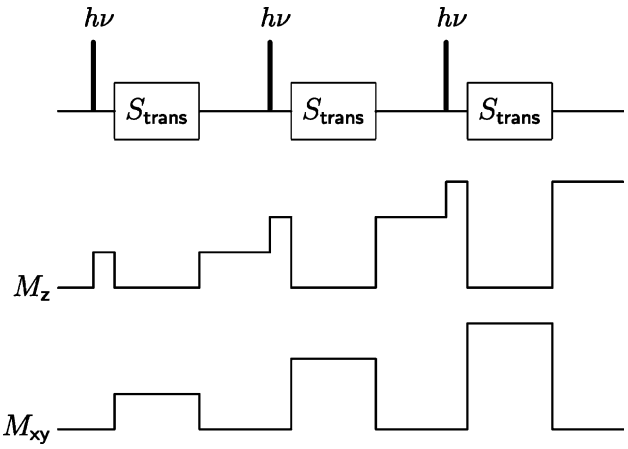

Fig. 1. Schematic representation of the timing (top trace) and the development of transverse and longitudinal magnetization, M_{xy} and M_z, in a multiflash time-resolved CIDNP experiment. The laser flashes are symbolized by *hν* and the transverse storage periods by the blocks marked S_{trans}. The longitudinal storage periods constitute all the rest of the pulse sequence, and have not been labeled explicitly.

it can be suppressed very efficiently by the storage cycles, as we will show.

3.2. Transverse storage

Fig. 2A displays the basic implementation of transverse storage, in which sampling is done with a π/2 pulse. This pulse is applied at the desired time Δt after the laser flash, and puts the CIDNP magnetization present at that instant completely into the transverse plane.

During the storage period S_1 chemical shift evolution is eliminated by spin echoes. Imperfections of the π pulses are compensated by employing the standard Carr–Purcell–Meiboom–Gill scheme [14,15]; an even number of echo pulses, phase-shifted by 90° with respect to the sampling pulse. The echo delays Δ_{e1} and Δ_{e2} have to be marginally different because of the background suppression scheme (see Section 3.3).

At the end of S_1, the transverse magnetization is flipped back to the z axis by another π/2 pulse, and is ready to be sampled again, together with the polarization newly generated by the next flash. Repetition rates, $1/t_{rep}$, of XeCl excimer lasers or Nd:YAG lasers, the two universally used systems for time-resolved CIDNP, are typically $(10\ \text{ms})^{-1}$ to $(100\ \text{ms})^{-1}$. Spin evolution under the influence of homonuclear J couplings for longer times within that range might lead to annoying phase distortions of multiplets. While these do not depend on Δt, and thus do not affect the kinetic evaluation, they can be avoided by shortening S_1 as far as possible and keeping the magnetization stored on the z axis (see Section 3.3) for the rest of the time until the next flash, i.e., for a duration S_2 such that $S_1 + S_2 = t_{rep}$.

After the last flash and sampling pulse, the accumulated signal can be acquired immediately or—allowing a more compact implementation of the pulse sequence, as displayed below, in Fig. 3—subjected to one more storage cycle as described and then read out by a π/2 pulse without a preceding flash.

Two constraints are imposed on the lower limits of the echo delays, i.e., of S_1.

One the one hand, no echo pulse should be applied before CIDNP has become constant on the timescale of that pulse, otherwise some unwanted polarization would be taken to the transverse plane at that stage, since any z magnetization not present for the whole duration of a π pulse experiences a flip angle smaller than 180°. When this constraint is violated, it becomes difficult or even impossible to extract the true kinetics

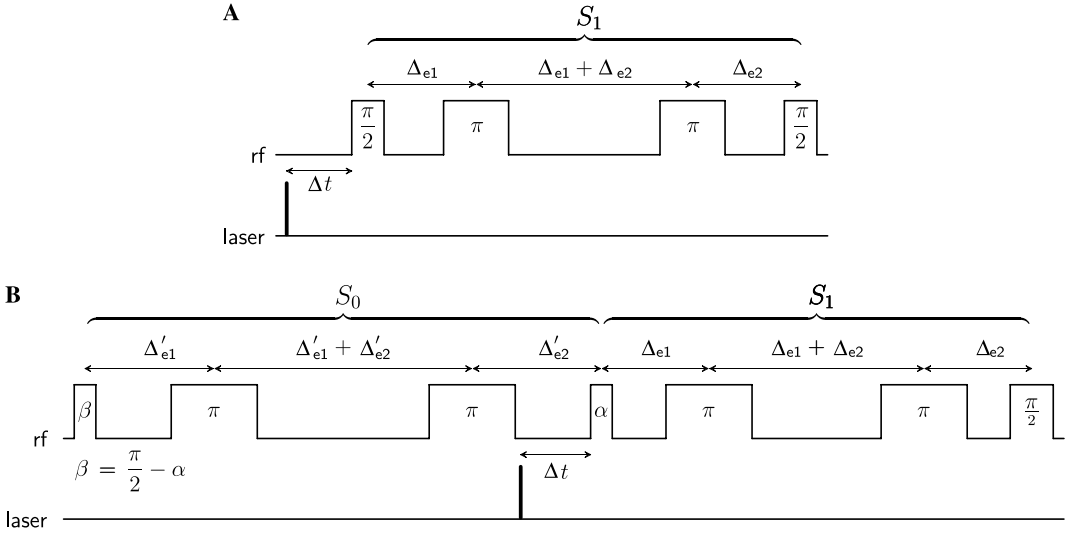

Fig. 2. Pulse sequences for temporary storage of transient CIDNP in the transverse plane when sampling is done with (A) a π/2 pulse, (B) a pulse of arbitrary flip angle α. These sequences are to be embedded in the longitudinal storage sequence shown in Fig. 3. Further explanation, see text.

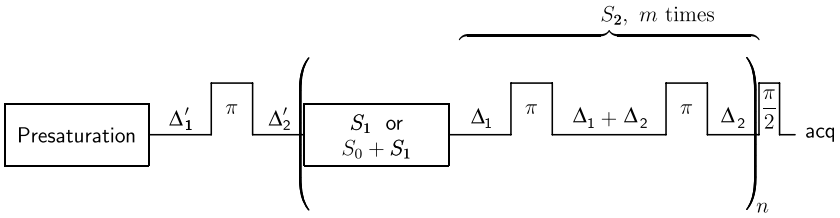

Fig. 3. Storage of transient CIDNP on the z axis (S_2) and background suppression in multiflash experiments. The first block denotes any presaturation scheme. The appropriate pulse sequence of Fig. 2 is inserted as the block labeled 'S_1 or $S_0 + S_1$,' the former corresponding to Fig. 2A, the latter to Fig. 2B. The double inversion S_2 is reiterated m times such as to make the total duration of the sequence enclosed in brackets equal to the laser repetition time t_{rep}; the enclosed part is repeated for each laser flash. Each π pulse is followed by a gradient pulse to destroy any transverse magnetization; these gradient pulses have been omitted for clarity. Further explanation, see text.

from the observed time dependences because the corrupting terms are *convolution integrals* of pulse and kinetics; fortunately, for protons it is very easily met because typical widths of π pulses are on the order of 10 μs, echo delays up to a millisecond will but rarely produce discernible multiplet distortions, and a chemical reaction that is fast on the former timescale will have long been completed on the latter.

On the other hand, CIDNP must have reached a stationary value before the magnetization is flipped back to the z axis. We stress that it is not necessary for it to become zero, since any z magnetization present at the moment of the flip-back pulse is taken to the transverse plane, where it can be destroyed by a pulsed field gradient; however, changes of the z magnetization during S_2 will be superimposed on the desired stored signal. Violation of this constraint is unavoidable in the rarer cases of extremely slow CIDNP kinetics but, again fortunately, the resulting distortion is only the *difference* of the CIDNP magnetizations at times $\Delta t + S_1 + S_2$ and $\Delta t + S_1$, so a correction is almost trivial, especially when the sampling times are chosen suitably.

The time resolution of CIDNP experiments is basically determined by the width of the RF sampling pulse. While deconvolution methods have been used to overcome this limitation [16], their success largely depends on the signal-to-noise ratio, so adaptation of the described scheme to shorter sampling pulses seemed highly desirable. With regard to the time-dependent magnetization, the building block of Fig. 2A can accommodate a shorter sampling pulse, of flip angle α, without any signal loss apart from the factor $\sin(\alpha)$; however, with regard to the stored magnetization that shorter pulse would be very inefficient because it utilizes only a fraction, all the rest being lost.

That problem is solved by the slightly more complex sequence displayed in Fig. 2B. Prior to the sampling pulse, the stored magnetization is first rotated towards the transverse plane by a pulse of flip angle $\pi/2 - \alpha$. A double spin echo leaves the residual z component unchanged and effects a refocussing of the transverse component at the moment of the sampling pulse. That pulse, therefore, takes the stored magnetization the rest of the way into the transverse plane. The laser flash is inserted into the interval between the second π pulse of the spin echo block and the sampling pulse, so CIDNP is not sampled by the preceding echo.

3.3. Background suppression and longitudinal storage

The whole transverse storage cycle is embedded in a background suppression and longitudinal storage scheme as displayed in Fig. 3.

Before the start of the pulse sequence proper, all background signals are destroyed, for instance by one or more π/2 pulses, each followed by a defocussing gradient. Subsequent partial recovery is unavoidable, but the background can easily be nulled at those points of time of the sequence when it would be harmful, i.e., whenever a pulse with a flip angle other than an integer multiple of 180° has to be applied. As one of us reported some time ago [18,19], this nulling can be achieved simultaneously for a wide range of relaxation times T_1 by inserting one or more π pulses, each preceded by a delay Δ_1 and followed by a delay Δ_2 with a fixed relationship between Δ_1 and Δ_2. One has to choose

$$\Delta_2 = T_{1,\min} \cdot \ln[2 - \exp(-\Delta_1/T_{1,\min})], \quad (1)$$

where $T_{1,\min}$ is the (known or estimated) minimum relaxation time of all the background. The effects of different relaxation times cancel to first order because nuclei relaxing faster recover a larger fraction of their equilibrium magnetization during Δ_1, so they have to start out from a more negative value at the beginning of Δ_2.

With the building block of Fig. 2A, background nulling has to occur at the moment of each π/2 pulse. For the first of these, this can be done by choosing Δ_1' and Δ_2' suitably. Background nulling at the moment of the second π/2 pulse is accomplished by adjusting the echo delays Δ_{e1} and Δ_{e2} according to Eq. (1).

To maintain the background suppression during S_2, an even number of π pulses is inserted with the appropriate timing (Δ_1 and Δ_2 in Fig. 3). Signal losses are minimized by employing composite pulses (GROPE-16) [17] for these inversions.

With the more complex building block of Fig. 2B, background suppression can be implemented just as easily as in the case of Fig. 2A, the only differences being that the delays of the pre-flash echo have to be adjusted in the same manner as those of the post-flash echo.

3.4. Validation

A chemical system that is suitable for assessing the performance of such multiflash pulse sequences has to fulfil two criteria. First, it should yield strong polarizations even in a conventional time-resolved CIDNP measurement because that control experiment provides the point of reference for a quantification of the signal enhancement. Second, it should exhibit a very high photostability because any sample degradation would, and the necessity of frequent sample changes might, make the assessment less reliable.

Both criteria are met almost ideally by a solution of the bicyclic amine diazabicyclo[2.2.2]octane (DABCO) in D_2O, with flavin mononucleotide (FMN) as the photosensitizer. The 12 equivalent DABCO protons are strongly polarized and yield a sharp singlet. The radical pairs are formed by a simple electron transfer [20], which is facile because the DABCO radical cation is highly stabilized by a two-centre three-electron bond; for that reason, quenching of the triplet precursor ^{3}FMN by DABCO competes favourably with quenching by oxygen, so CIDNP is easily observable in undegassed solutions as well. Unlike with other tertiary amines, hydrogen abstraction leading to irreversible product formation is impossible because the bicyclic structure prevents the hypothetical α-amino alkyl radical from adopting a conformation with a stabilizing orbital overlap between the lone pair on the nitrogen and the adjacent carbon-centered radical site. This makes the reaction ideally cyclic, the only products being the starting compounds FMN and DABCO, which are regenerated by reverse electron transfer. Even after several hundreds of flashes had been absorbed by the same sample, we were not able to detect a decrease of the DABCO polarization produced per flash.

The time dependence of CIDNP in this system is due to exchange cancellation [21]: the precursor multiplicity is triplet. The radical pair mechanism creates an absorptive polarization of the DABCO protons in the singlet pairs, and an emissive one in the triplet pairs. The singlet pairs recombine on a nanosecond timescale, so within the time resolution of the experiment there is an instantaneous absorption signal of the amine D. The emissive polarization (signified by a downward arrow) turns up in the escaping free radicals $D^{\bullet+}$ on the same timescale, and are then also transferred, but much more slowly, to D by an electron exchange with surplus starting material

$$^{\downarrow}D^{\bullet+} + D \rightarrow {}^{\downarrow}D + D^{\bullet+}. \quad (2)$$

The absorptive polarization $^{\uparrow}D$ present immediately after the flash is thus gradually cancelled by reaction Eq. (2), the rate of which is reflected by the time dependence of the CIDNP intensity.

Three further processes normally modify that simple scheme. First, the radical pairs are formed by bimolecular quenching of ^{3}FMN by DABCO, so for small amine concentrations an initial rise of the absorptive signal is observed, reflecting the slow formation of radical pairs. Second, nuclear spin relaxation in the free radicals destroys part of the polarization and makes the exchange cancellation incomplete, which leads to a residual absorption remaining at long times after the flash. Third, encounters of free radicals $FMN^{\bullet-}$ and $DABCO^{\bullet+}$ both transfer existing polarizations to the observed product and create new polarizations from F-pairs, resulting in much more complex CIDNP kinetics. To suppress all these effects, we increased the amine concentration to 50 mM. Under these conditions, the exchange process of Eq. (2) has a half-life of 36 μs and dominates the kinetics such that deviations from a simple first-order decay are no longer observable (see Fig. 4). By control experiments, we ascertained that the background suppression scheme can also accommodate this case, where the concentration of radical pairs—limited by the starting concentration of FMN, which is in turn constrained to about 0.1 mM by its optical absorption properties—is at least 500 times lower than the concentration of background molecules.

Fig. 4 shows a comparison of the decay curves, monitored over three half-lives, for the conventional time-re-

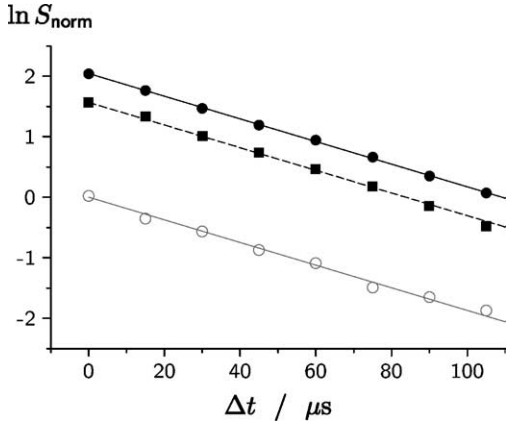

Fig. 4. Time-resolved CIDNP measurements on a sample of 0.1 mM FMN and 50 mM DABCO in D_2O, pH about 10. Dotted line and open circles, single-flash experiment, π/2 pulse for sampling; solid line and filled circle, 8 flashes and π/2 pulse; dashed line and solid squares, 8 flashes and pulse of flip angle 40°. Δt is the delay between the laser flash and the sampling RF pulse. All CIDNP signals S_{norm} were scaled to that at $\Delta t = 0$ in the single-flash experiment. Transverse storage periods (see Fig. 2) S_0 and S_1, 800 μs each; longitudinal storage period (see Fig. 3) S_2, 100 ms − S_0 − S_1, with $m = 1$. The actual values of all associated delays depend on the variable delay Δt (Fig. 2), and follow from Eq. (1).

solved CIDNP experiment and the multipulse schemes of the present work. It is obvious that the results are identical apart from the expected offset in the first-order plot, so the pulse sequences described do not distort the kinetics.

The considerable signal gain obtainable by the multiflash methods is demonstrated in Fig. 5. In that experiment, the delay between laser flash and sampling pulse was kept fixed, and a π/2 pulse was used for sampling (i.e., the pulse sequence of Fig. 2A was employed). With increasing number of flashes n, the signal is seen to rise slightly less than linearly. A quantitative evaluation of the signal-to-noise ratio as a function of the number of flashes, both for sampling with a π/2 pulse and a shorter pulse, is finally given in Fig. 6. In this figure, normalization was done with respect to the value obtained in a single-flash experiment with a π/2 pulse.

Two factors are expected to spoil a linear increase of the signal with the number of flashes. The most important in our case is thought to be nuclear spin relaxation during the storage periods. Our laser system does not permit repetition times t_{rep} shorter than 100 ms, so in a 10-flash experiment the signal has to be stored, on average, for as much as half a second. We emphasize that this does not constitute a fundamental limitation because lasers that are capable of firing much more rapidly are commercially available. In addition to relaxation, RF pulse imperfections might also cause some signal loss.

The combined effect of both relaxation and pulse imperfections can be represented by an efficiency factor b ($0 \leqslant b \leqslant 1$), which quantifies how much of the signal s generated by one flash as well as of the accumulated signal from the preceding flashes is retained in one storage cycle. Because the same relative amount is lost in each cycle, the final signal S in an n-flash experiment is obtained by summing up all contributions

$$S = s\sum_{j=1}^{n} b^j = sb\frac{1-b^n}{1-b}. \tag{3}$$

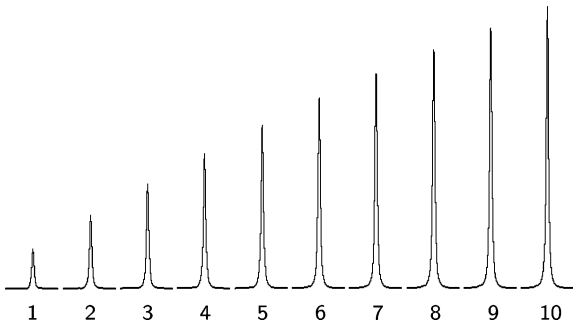

Fig. 5. CIDNP signals from a sample of 0.1 mM FMN and 50 mM DABCO in D_2O, pH about 10, obtained with the multiflash method described in Figs. 2A and 3 ($\Delta t = 0$). The number of flashes per acquisition is given below each trace. Transverse and longitudinal storage periods as in Fig. 4.

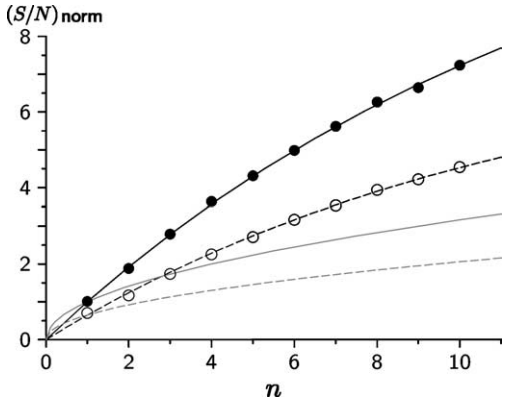

Fig. 6. Improvement of the sensitivity of time-resolved CIDNP experiments by multiflash methods and by signal averaging. Sample, 0.1 mM FMN and 50 mM DABCO in D_2O, pH about 10, $\Delta t = 0$. Transverse and longitudinal storage periods as in Fig. 4. Shown is the signal-to-noise ratio scaled to that in a single-flash one-acquisition measurement with a π/2 sampling pulse, $(S/N)_{norm}$; n is the number of flashes. Solid line and filled circles, multiflash experiments with π/2 sampling pulses; dashed line and open circles, multiflash experiments with 40° sampling pulses; grey solid and dotted line without data points, n single-flash experiments coadded, π/2 and 40° sampling pulses, respectively. The fit curves through the data points are explained in the text. Best-fit parameters, 0.93 (π/2 pulses) and 0.92 (40° pulses).

The parameter b can be written as

$$b = b' \exp(-t_{rep}/T_{1,eff}) \tag{4}$$

with b' describing the effect of all nonidealities and $T_{1,eff}$ being an effective relaxation time (i.e., the average of the true T_1 and of T_2 weighted with the durations of the longitudinal and transverse storage periods). The presence of a considerable amount of transient radicals is expected to shorten $T_{1,eff}$ in Eq. (4) compared to T_1 measured in the absence of irradiation. For the same reason, experiments as in Fig. 6 on a series of molecules with different T_1 times are not expected to permit a reliable separation of relaxation and pulse imperfection effects. The best way to achieve that would be by varying t_{rep} while retaining all other parameters because this will only change the relaxation loss but leave the nonidealities unaffected. Unfortunately, with our laser such a variation was not feasible.

Instead, we took the following approach. The relaxation loss $\exp(-t_{rep}/T_1)$ must be identical for the pulse sequences of Figs. 2A and B because both are imbedded into the same period of time t_{rep}. Any differences in the efficiency factor b must, therefore, be ascribed to nonidealities, and will allow an estimate of how important these effects are. The curves through the data points of Fig. 6 show a simultaneous fit of Eq. (3) to the results of sampling with a π/2 pulse (Fig. 2A) and a pulse of 40° flip angle (Fig. 2B). For this fit, we set the ratio of the two s values to the theoretical ratio sinα and kept it fixed, but treated the b values as free parameters.

It is assumed that the losses in the inversion part S_2 of the sequences are negligible because the GROPE-16 pulses are known to have extremely good efficiencies; this was also verified experimentally. The ratio of the b values should thus reflect the losses caused by the additional spin echo part S_0 in the second sequence. The result indicates a loss due to pulse imperfections on the order of one percent per echo block, which is not very severe. The relaxation loss in this system is approximately 6% per storage cycle, corresponding to an effective relaxation time of 1.6 s. As expected, if relaxation is accelerated by the presence of the radicals, this is slightly shorter than T_1 of the sample without laser irradiation, which was measured to be 1.76 s.

Further corroboration of these concepts was obtained from experiments as in Fig. 6 on the ^{19}F signal of 4-fluorophenol, again with FMN as the photosensitizer. For that system, where a different probe had to be used, the results with a $\pi/2$ sampling pulse and with a $\pi/4$ sampling pulse could be fitted with exactly the same value of b, which indicates that the deviations in the previous case are probe-specific, i.e., originate from pulse nonidealities.

Despite the losses, the gain in the signal, and thus in the signal-to-noise ratio, still amounts to a factor of more than 7 with 10 flashes per acquisition, as Fig. 6 shows. With a faster laser, this could be brought still nearer to the linear regime; for example, on the basis of the fits a value of 9 is calculated for $t_{rep} = 10$ ms. The signal-to-noise ratio can, of course, also be improved in the usual way, by signal averaging. Total experimental time is not normally a limiting factor in time-resolved CIDNP measurements, but sample photostability is, and often necessitates sample changes during an experiment with all the accompanying reproducibility problems. As their main advantage, therefore, the multiflash schemes allow one to obtain the same signal-to-noise ratio with fewer flashes. To illustrate that point, the theoretical curves for the signal-to-noise ratio in n averaged one-flash experiments have also been included in the figure. Compared to them, the multiflash experiments in a limiting loss-free situation would either yield the same signal-to-noise ratio with $\sqrt{n}$ flashes instead of n, or a signal-to-noise ratio that is higher by $\sqrt{n}$ for the same number of flashes. Even in our case, where there are some losses, the improvement is substantial.

Acknowledgments

Financial support from the BBSRC and INTAS (Project No. 02-2126) and the DFG (Grants Go 615/6-3 and Go 615/9-1) is gratefully acknowledged. I.K. thanks the Scatcherd European Foundation and the Hill Foundation for a PhD studentship.

References

[1] R.R. Ernst, W.A. Anderson, Application of Fourier transform spectroscopy to magnetic resonance, Rev. Sci. Instrum. 37 (1966) 93–102.
[2] W.P. Aue, E. Bartholdi, R.R. Ernst, Two-dimensional spectroscopy. Application to nuclear magnetic resonance, J. Chem. Phys. 64 (1976) 2229–2246.
[3] J. Bargon, H. Fischer, U. Johnsen, Nuclear magnetic resonance emission lines during fast radical reactions. I. Recording methods and examples, Z. Naturforsch. A 22 (1967) 1551–1555.
[4] G.L. Closs, Mechanism explaining nuclear spin polarizations in radical combination reactions, J. Am. Chem. Soc. 91 (1969) 4552–4554.
[5] R. Kaptein, L.J. Oosterhoff, Chemically induced dynamic nuclear polarization. II. Relation with anomalous ESR spectra, Chem. Phys. Lett. 4 (1969) 195–197.
[6] See, e.g. M. Goez, Photochemically induced dynamic nuclear polarization, in: D.C. Neckers, D.H. Volman, G. von Bünau (Eds.), Advances in Photochemistry, vol. 23, Wiley, New York, 1997, pp. 63–164, and references therein.
[7] M. Goez, J. Rozwadowski, B. Marciniak, CIDNP-spectroscopic observation of $(S^{\therefore +}N)$ radical cations with a two-center three-electron bond during the photooxidation of methionine, Angew. Chem. Int. Ed. Engl. 37 (1998) 628–630.
[8] H.D. Roth, Magnetic resonance studies and ab initio calculations as structure probes for radical cations—hexa-1,5-diene systems, Z. Phys. Chem. 180 (1993) 135–158.
[9] H.D. Roth, T. Herbertz, P.S. Lakkaraju, G. Sluggett, N.J. Turro, Oxidation of arylcyclopropanes in solution and in a zeolite: structure and rearrangements of the phenylcyclopropane radical cation, J. Phys. Chem. A 103 (1999) 11350–11354.
[10] P.J. Hore, R.W. Broadhurst, Photo-CIDNP of biopolymers, Prog. NMR Spectrosc. 25 (1993) 345–402.
[11] K.H. Mok, P.J. Hore, Photo-CIDNP methods for studying protein folding, Methods 34 (2004) 75–87.
[12] S. Schäublin, A. Wokaun, R.R. Ernst, Pulse techniques applied to chemically induced dynamic nuclear polarization, J. Magn. Reson. 27 (1977) 273–302.
[13] G.L. Closs, R.J. Miller, Laser flash photolysis with NMR detection. Microsecond time-resolved CIDNP: separation of geminate and random-phase processes, J. Am. Chem. Soc. 101 (1979) 1639–1641.
[14] H.Y. Carr, E.M. Purcell, Effects of diffusion on free precession in nuclear magnetic resonance experiments, Phys. Rev. 94 (1954) 630–638.
[15] S. Meiboom, D. Gill, Modified spin-echo method for measuring nuclear relaxation times, Rev. Sci. Instrum. 29 (1958) 93–102.
[16] M. Goez, Evaluation of flash CIDNP experiments by iterative reconvolution, Chem. Phys. Lett. 165 (1990) 11–14.
[17] A.J. Shaka, R. Freeman, Composite pulses with dual compensation, J. Magn. Reson. 55 (1983) 487–493.
[18] M. Goez, Pseudo steady-state photo-CIDNP measurements, Chem. Phys. Lett. 188 (1992) 451–456.
[19] M. Goez, Pseudo steady-state photo-CIDNP measurements with improved background suppression, Appl. Magn. Reson. 5 (1993) 113–126.
[20] G. Porcal, S.G. Bertolotti, C.M. Previtali, M.V. Encinas, Electron transfer quenching of singlet and triplet excited states of flavins and lumichrome by aromatic and aliphatic electron donors, Phys. Chem. Chem. Phys. 5 (2003) 4123–4128.
[21] G.L. Closs, E.V. Sitzmann, Measurements of degenerate radical ion–neutral molecule electron exchange by microsecond time-resolved CIDNP. Determination of the relative hyperfine coupling constants of chlorophylls and derivatives, J. Am. Chem. Soc. 103 (1981) 3217–3219.